Dear Author,

Please, note that changes made to the HTML content will be added to the article before publication, but are not reflected in this PDF.

Note also that this file should not be used for submitting corrections.

Physics and Chemistry of the Earth xxx (2015) 1–8

Contents lists available at ScienceDirect

Physics and Chemistry of the Earth

journal homepage: www.elsevier.com/locate/pce

The LF radio anomaly observed before the $M_w = 6.5$ earthquake in Crete on October 12, 2013

Tommaso Maggipinto [a, *], Pier Francesco Biagi [a], Roberto Colella [a], Luigi Schiavulli [a], Teresa Ligonzo [a], Anita Ermini [b], Giovanni Martinelli [c], Iren Moldovan [d], Hugo Silva [e], Michael Contadakis [f], Christos Skeberis [f], Zaharias Zaharis [f], Emmanuel Scordilis [g], Konstantinos Katzis [h], Aydın Buyuksarac [i], Sebastiano D'Amico [j]

[a] University of Bari, Department of Physics, Bari, Italy
[b] Department of Industrial Engineering, University of Tor Vergata, Rome, Italy
[c] Arpa Emilia Romagna, Reggio Emilia, Italy
[d] National Institute of Earth's Physics, Seismological Department, Bucharest, Magurele, Romania
[e] Geophysical Centre of Évora and Physics Department, ECT, University of Évora, Portugal
[f] Department of Surveying & Geodesy, University of Thessaloniki, Thessaloniki, Greece
[g] Department of Geophysics, University of Thessaloniki, Thessaloniki, Greece
[h] Department of Computer Science and Engineering, European University Cyprus, Nicosia, Cyprus
[i] Department of Geophysics, Canakkale Onsekiz Mart University, Canakkale, Turkey
[j] Department of Physics, University of Malta, Malta

ARTICLE INFO

Article history:
Received 13 October 2014
Received in revised form
6 October 2015
Accepted 8 October 2015
Available online xxx

Keywords:
Earthquake radio precursor
LF precursors

ABSTRACT

On October 12, 2013, an earthquake with $M_w = 6.5$ occurred in the southern Hellenic Arc, approximately 20 km off the west coast of Crete. The main shock, the focal depth of which is on the order of 40 km, was followed by aftershocks felt in the nearby cities and villages, although the aftershock sequence was poor. The epicentre was located at approximately 60 km from a radio receiver in Crete (CRE), which belongs to the European VLF/LF Radio Network. Several days before the earthquake, a clear disturbance occurred in one of the ten radio signals that the CRE receiver sampled. The disturbance, which can be considered an anomaly, appeared in the 216 kHz radio signal radiated by the Radio Monte Carlo (MCO) transmitter. The radio path MCO-CRE crossed directly over the epicentre area of the aforementioned earthquake. In this work, we present a detailed analysis of the MCO signal anomaly using spectral tools. We also investigate the behaviour of other radio signals sampled by the CRE receiver and consider other possible causes of disturbances on the MCO radio signal. We conclude that the disturbance in the MCO radio signal is a convincingly possible precursor of the earthquake in Crete. Emission of electromagnetic waves with a frequency band that includes 216 kHz from the focal zone of the earthquake can provide a satisfactory explanation of the radio anomaly.

1. Introduction

Very-Low-Frequency (VLF) radio signals lie in the 20–60 kHz frequency band. These radio signals are used for worldwide navigation support such as timing signals and military purposes. These signals propagate in the earth-ionosphere wave-guide zone along great circle propagation paths. Low-Frequency (LF) radio signals lie in 150–300 kHz frequency band and are used for long-way broadcasting by few transmitters around the world (this type of broadcasting is gradually going out of use). VLF/LF radio signal propagation is affected by different factors such as meteorological conditions, solar bursts and geomagnetic activity. In addition, variations of some parameters in the ground, atmosphere and ionosphere during the preparatory phase of an earthquake can produce disturbances in the VLF/LF signals. As reported in many previous studies (Biagi et al., 2001a,b; Biagi and Hayakawa, 2002; Biagi et al., 2004, 2005; 2006, 2008; Hayakawa and Sato, 1994; Hayakawa et al., 1996, 2006; 2010; Morgounov et al., 1994; Molchanov and

* Corresponding author. Department of Physics, University of Bari, Via Amendola 173, 70126 Bari, Italy.
E-mail address: tommaso.maggipinto@uniba.it (T. Maggipinto).

http://dx.doi.org/10.1016/j.pce.2015.10.010
1474-7065/

Hayakawa, 1998; Molchanov et al., 2006; Rozhnoi et al., 2004, 2005; 2006, 2007; 2009), these disturbances are classified as anomalies; different analysis methods such as the residual dA/dP (Rozhnoi et al., 2004), terminator time TT (Hayakawa et al., 1996), Wavelet spectra and Principal-Component Analysis have been used (Biagi et al., 2006, 2008).

In this paper, we analyse some sampled LF signals in the framework of the European radio network, and using the Wavelet analysis, we investigate possible connections between anomalies in the radio signals and the $M_w = 6.5$ earthquake in Crete on October 12, 2013.

2. The European Radio Network

Since 2000, Japanese researchers have been able to rely on a VLF radio network (the Pacific network), which has seven receivers to measure the intensity and phase of VLF radio signals from two different transmitters. On February 2002, in the framework of a scientific cooperation among Japanese, Russian and Italian teams, a receiver was placed into operation in the Department of Physics at the University of Bari, which marked the beginning of the development of a European network. In 2008, a new receiver that can work with both VLF and LF signals was developed by the Italian factory Elettronika (Palo del Colle, Bari). Since then, several receivers of the new type have been installed in different places around Europe, and the current status of the network is reported in Fig. 1. Some peculiarities of the transmitters are listed in Table 1.

It is important to note that the epicentre of the Crete earthquake is notably near the receiver in Crete. Fig. 1 also shows ten sampled VLF/LF radio signals (in the 5th Fresnel zones) in Crete.

Table 1
Peculiarities of the VLF and LF transmitters of the European Radio Network.

Label	Country	Power (kW)	Frequency (kHz)
VLF transmitters			
GBZ	United Kingdom		19.58
ICV	Sardinia, Italy		20.27
HWU	France		21.75
DHO	Germany		23.40
NRK	Iceland		37.50
ITS	Sicily, Italy		45.90
LF transmitters			
RRO	Romania	1200	153
FRI	France	2000	162
TRT	Turkey	1200	180
EU1	Germany	2000	183
CH1	Algeria	2000	198
MCO	France	1200	216
RRU	Russia	2500	261
CZE	Czech Republic	500	270

3. The $M_w = 6.5$ Crete earthquake

The Hellenic Arc, which is the margin along which the Eurasian and Mediterranean plates collide, is dominated by low-angle thrust faults. This thrust-faulting zone, which follows the Hellenic trench, is in the southwestern part of this margin (Papazachos and Delibasis, 1969). The faults of this zone, which exhibit the NW–SE direction and dip towards NE, i.e., toward the concave side of the arc (Aegean), are responsible for the generation of strong, mostly shallow earthquakes. The strongest shallow earthquake of the entire Mediterranean area occurred in this zone on July 21, 365 AD with M = 8.3 (Papazachos and Papazachou, 2003). This earthquake generated the highest tsunami of the Mediterranean and caused a

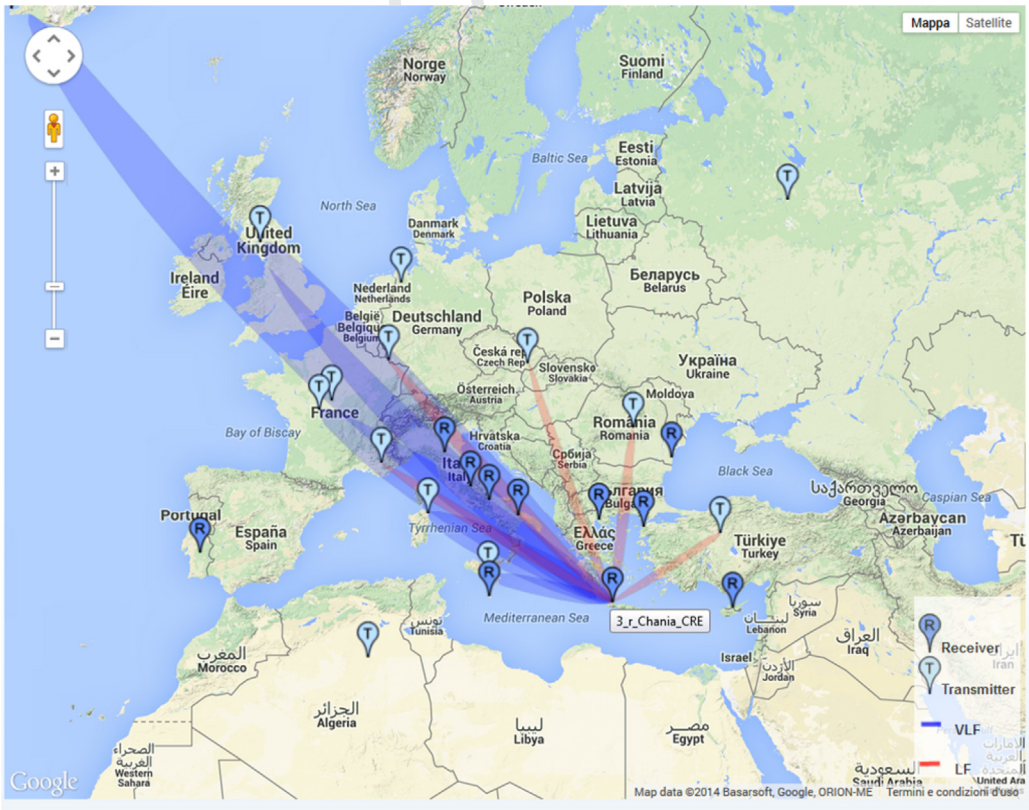

Fig. 1. Map of different receivers and the VLF and LF transmitters of the European Radio Network. The blue (VLF) and red (LF) ellipses represent the 5th Fresnel zones of the signals received in Crete. (For interpretation of the references to colour in this figure legend, the reader is referred to the web version of this article.)

Please cite this article in press as: Maggipinto, T., et al., The LF radio anomaly observed before the $M_w = 6.5$ earthquake in Crete on October 12, 2013, Physics and Chemistry of the Earth (2015), http://dx.doi.org/10.1016/j.pce.2015.10.010

remarkable uplift of the western coast of Crete, which ranged between 0 and 9 m and was observed along a distance of more than 100 km (Thommeret et al., 1981; Pirazzoli et al., 1982).

The M_w = 6.5 earthquake of October 12, 2013 (Fig. 2) was generated by a thrust fault striking NW–SE; the seismic fault is located at a relatively small depth at the early stage of the formation of the Wadati-Benioff zone (Papazachos and Comninakis, 1970, 1971; Papazachos et al., 2000), which is propagating at bigger depths to the NE. This fault belongs to the thrust-faulting zone described above and is actually a part of the seismogenic fault of the strong earthquake of 365 AD. The focal depth of the earthquake is of the order of ~40 km, as shown in the reports of seismological centres and quick moment tensor solutions (see www.emsc-csem.org), which characterized it as a shallow event. This characterization is also supported by the aftershocks following the main shock (Fig. 2), which were felt in the nearby cities and villages, although the aftershock sequence was poor (data till the end of November 2013).

4. Data analysis

4.1. Raw radio data and preliminary investigation

In Fig. 3, the intensity raw data of the five LF radio signals that the CRE receiver collected is reported for the time period from the middle of July till the end of October 2013. The sampling time is 1 min, and the radio signal intensity on the vertical axis is expressed in dB_m with $dB_m = 20\log_{10}(V_{pp,\,mV})$, where $V_{pp,\,mV}$ is the peak-to-peak value in mV. The general features of the signals are the standard ones with high level at night time and low level at day time. Fig. 3 indicates that an anomalous behaviour appeared in the MCO-216 kHz signal (this signal can be well received, primarily at night, in the entire continent of Europe) immediately before the Crete earthquake, the occurrence of which is indicated by the vertical red line. The anomaly started at the beginning of October and lasted approximately 7 days. Two smaller anomalies can be observed in approximately August and after the occurrence of the earthquake, which are linked to peculiar meteorological conditions along the path of the MCO signal. The remaining four LF signals appear unaffected by any sort of perturbation.

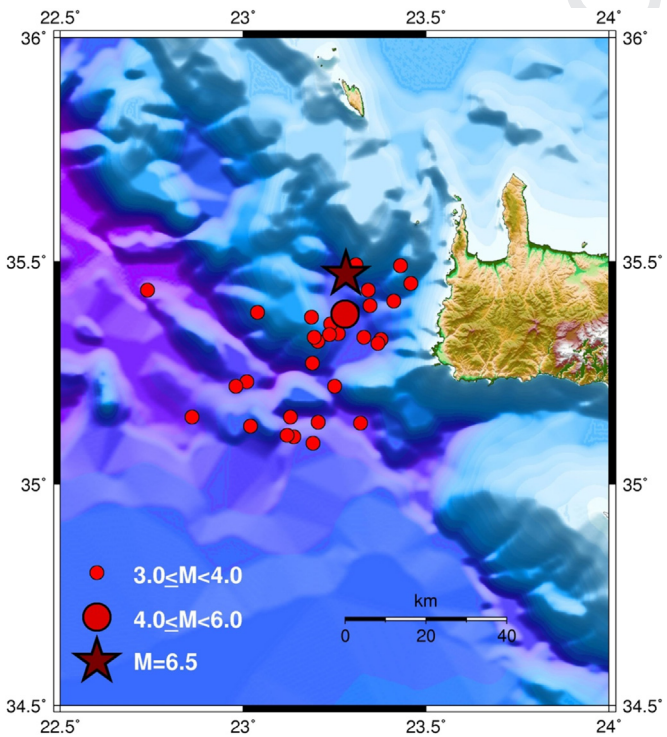

Fig. 2. Geographical distribution of the aftershocks, which were recorded till the end of November 2013 (red circles), of the October 12, 2013, M = 6.5 main shock (denoted by a star) in the SW part of the Hellenic arc, ~20 km off the west coast of Crete. (For interpretation of the references to colour in this figure legend, the reader is referred to the web version of this article.)

The fact that only one of five signals was perturbed eliminates the possibility that the anomaly was connected to a faulty running of the receiver in the LF band. In addition, the possibility of a faulty running of the transmitter was excluded, as reported in section 4.3. Thus, connections with disturbances in the global geomagnetic activity appear unlikely. However, we checked the geomagnetic indices (www.ngdc.noaa.gov/stp/geomag/geoib.html), and in the time interval of the radio anomaly, no particular geomagnetic activity appears. Nonetheless, the anomaly might be related to adverse meteorological condition around the receiver location along the direction of the MCO radio path. To verify this possibility, the meteorological data in Greece were examined, but no particular situation was noticed.

Then, to study the anomalous feature in the mentioned MCO radio signal, the data collected by the Crete receiver were tested using the Wavelet analysis.

4.2. Principles of wavelet analysis

The Wavelet transform enables one to highlight the spectral components of a signal using variable-width time windows and by considering that the frequency content of these windows is inversely related to the time widths; thus, the signal localization is simultaneously obtained in both time and frequency (Daubechies, 1992; Strang and Nguye, 1996). Thus, the wavelet transform is an excellent tool to analyse the time series that contain non-stationary power at many different frequencies. To highlight the essential features of the method (Torrence and Compo, 1998 and references therein), assume that one has a time series x_n with equal time spacing dt and $n = 0 \ldots N-1$. In addition, assume that one has a *wavelet function* $\psi_0(\eta)$; to be admissible as a wavelet, this function must have zero mean and be localized in both time and frequency space. An example is the Morlet wavelet, which consists of a Gaussian-modulated plane wave:

$$\psi_0(\eta) = \pi^{-1/4} e^{i\omega_0\eta} e^{-\eta^2/2} \tag{1}$$

The continuous wavelet transform of a discrete sequence x_n is defined as the convolution of x_n with a scaled and translated version of $\psi_0(\eta)$:

$$W_n(s) = \sum_{n'=0}^{N-1} x_{n'} \psi^* \left[\frac{(n'-n)dt}{s}\right] \tag{2}$$

where (*) indicates the complex conjugate. By varying the *wavelet scale* s and moving along the *localized time index* n, one can construct a picture of both the amplitude of any feature versus the scale and how this amplitude varies with time. The subscript 0 on ψ is dropped to indicate that this ψ is also normalized (Torrence and Compo, 1998). Then, one can define the *wavelet power spectrum* as $|W_n(s)|^2$. The power spectrum can be represented as a two-dimensional plot, which provides information on the strength and precise time of occurrence of various Fourier components in the original time series after the plot is properly normalized with respect to the power of the white noise. Generally, colour ranging from blue to red indicates an increase in power strength; thus, the red zones define the anomalies (Biagi et al., 2008). The relationship

Please cite this article in press as: Maggipinto, T., et al., The LF radio anomaly observed before the M_w = 6.5 earthquake in Crete on October 12, 2013, Physics and Chemistry of the Earth (2015), http://dx.doi.org/10.1016/j.pce.2015.10.010

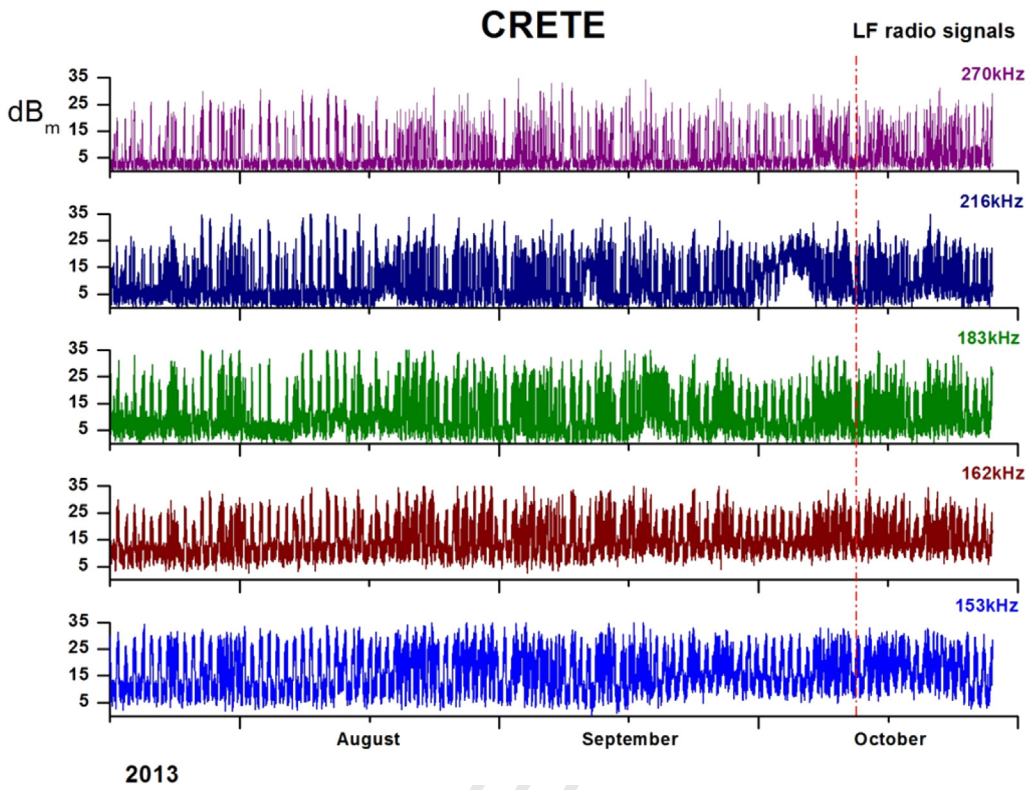

Fig. 3. Intensity raw data of the CZE (270 kHz), MCO (216 kHz), EU1 (183 kHz), (162 kHz) and RRO (153 kHz) radio signals collected by the CRE receiver from the middle of July 2013 till the end of October 2013. The sampling rate at which raw data were recorded is 1 datum per minute. As described in the main text, dB_m is reported on the vertical axis.

between the *equivalent Fourier period* and the wavelet scale can be analytically derived for a particular wavelet function. For the Morlet wavelet with $\omega_0 = 6$, $\tau = 1.03\ s$, where τ is the Fourier period, which indicates that for the Morlet wavelet, the wavelet scale is almost equal to the Fourier period.

After a wavelet function is selected, it is necessary to select a set of scales s to use in the wavelet transform. It is convenient to write the scales as fractional powers of two:

$$s_j = s_0 2^{j\delta j}, \quad j = 0, 1, \ldots, J \quad \text{with} \quad J = (\delta j)^{-1} \log_2(Ndt/s_0) \qquad (3)$$

where s_0 is the smallest resolvable scale, and J determines the largest scale; s_0 should be selected such that the equivalent Fourier period is approximately $2\delta t$. The choice of a sufficiently small δj depends on the width in the spectral space of the wavelet function. For the Morlet wavelet, δj ~0.5 is the largest value that provides adequate sampling in scale, whereas for other wavelet functions, a larger value can be used. Smaller values of δj provide finer resolutions.

In this study, we adopted the Morlet function as the Wavelet function (1).

Generally, because of different conditions of the ionosphere, VLF/LF radio signals are less disturbed during the night than during the day. Hence, in previous studies to reveal seismic anomalies, the radio data were mainly analysed based on the night-time data. In this study, we selected the identical approach. As a first step, the radio data considered in this study were separated into day-time data and night-time data, where the night-time window is from 0.00 to 03.00 (UT). Because the sampling time is 1 min, when we consider only night-time data, we have a time series of 180 data points per day. Then, the night-time series was analysed using the wavelet analysis with the following choice of parameters: $dt = 1/180$, $s_0 = 2\ dt$ and $\delta j = 0.025$. This value of δj appears adequate to provide a fine-resolution picture of the wavelet power.

4.3. Wavelet analysis of the radio data

First, the sampled MCO-216 kHz signal in Crete was analysed. Fig. 4 shows the results of the Wavelet analysis on the night-time data. We converted the wavelet scale into the corresponding Fourier period, and we report the power spectrum in the top panel. A clear anomaly is observed with a spectral content of approximately 20 days, which appeared some days before the earthquake. A comment regarding the spectral content of the anomaly is necessary: in (Biagi et al., 2008), the anomaly had a duration of less than one day; thus, appropriate Fourier periods to be investigated were in the band of 60–120 min. In this case, the duration of the anomaly is several days, and the appropriate periods to be investigated are in the range of 4–32 days. Because the colour scale in the wavelet power spectrum picture is only indicative, the bottom panel of Fig. 4 shows the power profile of the Fourier period for which the maximum power is identified, similarly to previous analyses (Biagi et al., 2008). In other words, the profile was obtained along the white line in the top panel. The vertical axis of the bottom panel is expressed in arbitrary units. Basically, the identical scenario appears if we analyse the data of the entire day instead of only the night-time data. It should be noted that the path of the considered signal is the only one among several LF paths that passes just over the epicentre of the earthquake as inferred from Fig. 1. To check the possibility that the anomaly could be related to some issue that affected the signal itself, e.g., variation in the broadcasting antenna, we analysed the identically collected MCO radio data in another receiver (IT-Tc) in Santeramo (southern Italy). Fig. 5 shows the results of the Wavelet analysis in this case, and no corresponding anomaly was found; a different anomaly, which is related to the meteorological condition at the receiver site,

Please cite this article in press as: Maggipinto, T., et al., The LF radio anomaly observed before the $M_w = 6.5$ earthquake in Crete on October 12, 2013, Physics and Chemistry of the Earth (2015), http://dx.doi.org/10.1016/j.pce.2015.10.010

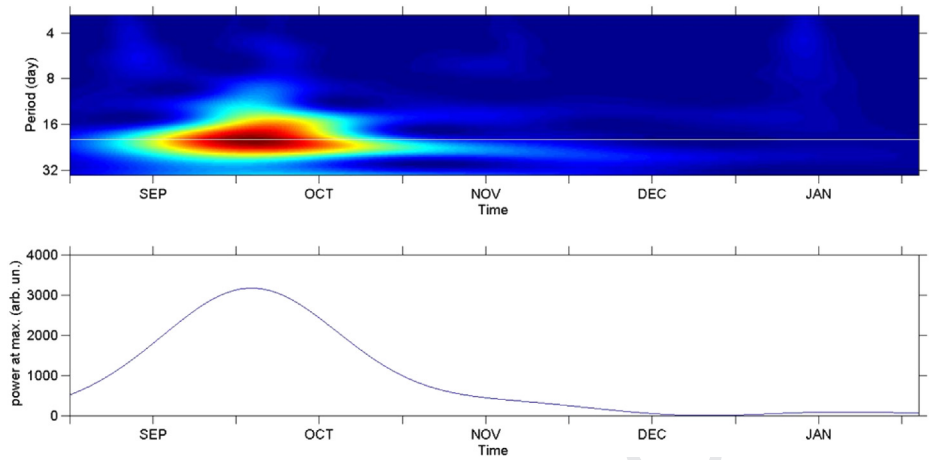

Fig. 4. Top panel: night-time spectrogram of the MCO (216 kHz) radio signal, which was collected by the CRE (Crete) receiver, from September 1, 2013 to February 5, 2014. Bottom panels: wavelet power that corresponded to the Fourier period when the maximum power was found.

appeared at the end of December. Moreover, the bottom panel of Fig. 5 shows that the power intensity spectrum is much lower than that at the CRE receiver.

The directionality of the effect of a seismic perturbation was verified by studying other collected signals in Crete. We expect that if we consider a signal whose radio path does not cross the epicentre area, it should be much less affected by the perturbation, which is indeed true in Figs. 6 and 7, where the Wavelet spectrum of CZE-270 kHz and RR0-153 kHz (Fig. 1 and Table 1) radio signals are reported, respectively. Apart from some effect during December–January because of meteorological conditions, in the period before the earthquake, we only observed a weak effect on the Fourier period for approximately 8 days. Considering that the CRE receiver is near the place of occurrence of the earthquake, the weak anomalies in CZE and RRO are consistent with disturbances in the focal zone, which can significantly affect the radio signal (MCO) that passed over the epicentre and radio signals (CZE and RRO) in the nearby areas to a lesser extent.

4.4. Statistical analysis

To strength the belief that the anomaly may be related to the Crete earthquake, first, let us evaluate the probability of the corresponding null hypothesis, i.e., the earthquake coincidentally occurred in 10 days from the onset of the detected anomaly. First, let us consider the probability that the earthquake accidentally occurs in k days from the onset of the anomaly in the radio signal during an N-days time interval. Let N be the duration of the time interval (days), t_1 is the starting day of the anomaly in the radio signal (event #1), and t_2 is the day of the occurrence of the seismic event (event #2).

We can assume that one anomaly and one earthquake occur during the time interval and consider that the two events are statistically independent.

Thus, the probability that event #2 can accidentally occur in k days from event #1 is calculated as follows:

$$P_k = P(0 < t_2 - t_1 \leq k) = \frac{k(N-k) + (k-1) + (k-2) + \ldots + 1}{(N-1) + (N-2) + \ldots + 1} \quad (4)$$

and for k = 10 and N = 180, we have $P_{10} = 11\%$.

Let us now consider that during the past 40 years, approximately 60 earthquakes with magnitude >5.0 occurred near Crete (data from USGS); this value is equivalent to a mean frequency of 1.5 earthquake per year or a probability per day of $P_e = 1.5/$

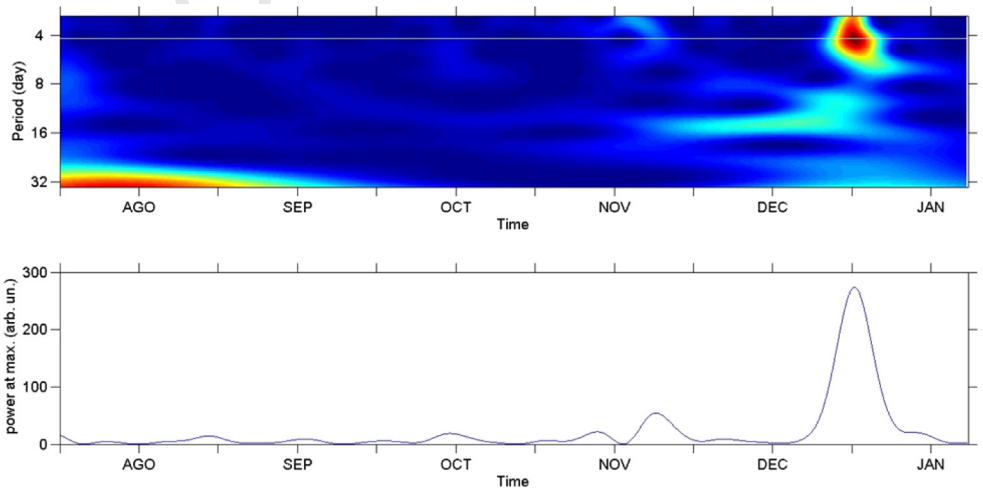

Fig. 5. Top panel: night-time spectrogram of the MCO (216 kHz) radio signal collected by the IT-Tc (southern Italy) receiver from August 1, 2013 to February 5, 2014. Bottom panels: wavelet power profile corresponding to the Fourier period when the maximum power was found.

Please cite this article in press as: Maggipinto, T., et al., The LF radio anomaly observed before the $M_w = 6.5$ earthquake in Crete on October 12, 2013, Physics and Chemistry of the Earth (2015), http://dx.doi.org/10.1016/j.pce.2015.10.010

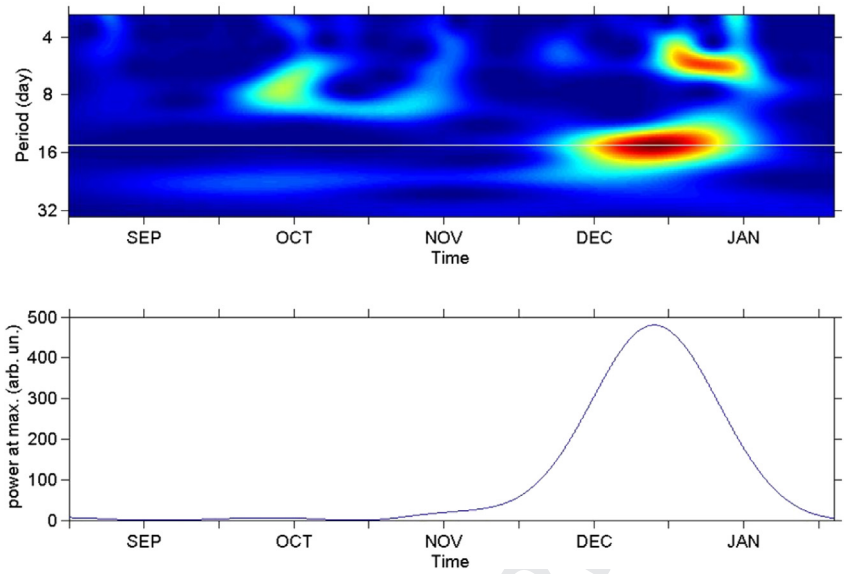

Fig. 6. Top panel: night-time spectrogram of the CZE (270 kHz) radio signal collected by the CRE receiver from September 1, 2013 to February 5, 2014. Bottom panels: wavelet power profile corresponding to the Fourier period when the maximum power was found.

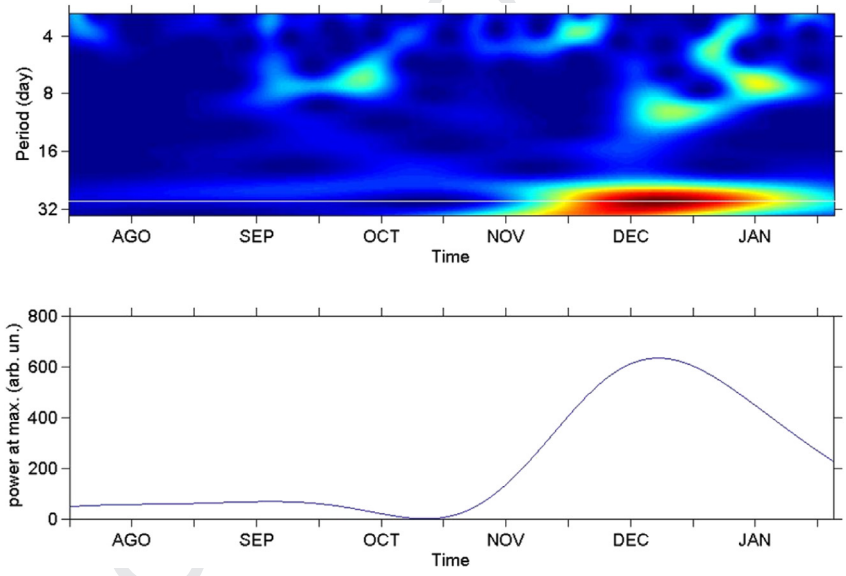

Fig. 7. Top panel: night-time spectrogram of the RRO (153 kHz) radio signal collected by the CRE receiver from August 1, 2013 to February 5, 2014. Bottom panels: wavelet power profile corresponding to the Fourier period when the maximum power was found.

$365 \approx 4 \times 10^{-3}$ in the frequentist approach. Therefore, our estimate of the order of magnitude of the joint probability for the earthquake and anomaly (occurring in 10 days) is P(earthquake ∩ anomaly in 10 days) = $P_{e,} \cdot P_{10} = 10^{-1}$–$10^{-2}$. Thus, we can reject the hypothesis that the earthquake occurs in 10 days from the MCO radio anomaly committing an error lower than 10^{-1}.

5. Discussion

Based on the previous results, the possibility that the anomaly in the sampled MCO signal in Crete is a precursor of the Crete earthquake is consistent. In addition, we note that since 2010, i.e., when systematic observations began, this anomaly is the first that occurred for an earthquake with M_w greater than 6, the epicentre of which is located near a receiver.

Now, let us propose a possible genesis of the radio anomaly that we have presented here.

A VLF/LF radio anomaly is produced by disturbances in the medium where radio signals are propagating; two different models have been proposed to justify these disturbances. The first model assumes a direct effect because of gases (mainly radon), aerosol or electromagnetic emissions from the crust during the preparatory phase of an earthquake (Alperovitch, 1997; Biagi, 1999; Biagi et al., 2001b; Hayakawa and Sato, 1994; Pulinets et al., 1998). The second model assumes an indirect effect, which is the appearance of gravity waves in the atmosphere-ionosphere (Hayakawa et al., 1996; Molchanov and Hayakawa, 1998) that pre-seismic phenomena in the ground produce as an intensification of the microfracturing processes and/or changes in existing fissures in the rocks. In both cases, an ionosphere-atmosphere-lithosphere

Please cite this article in press as: Maggipinto, T., et al., The LF radio anomaly observed before the $M_w = 6.5$ earthquake in Crete on October 12, 2013, Physics and Chemistry of the Earth (2015), http://dx.doi.org/10.1016/j.pce.2015.10.010

coupling is assumed. In Fig. 3, the MCO radio anomaly appears as an increase of the signal intensity; generally, other radio anomalies in previous cited works consist of decreases in signal intensity because the conditions of signal propagation into the medium worsen because of the aforementioned effects. Thus, the anomaly in the MCO radio signal must be explained in terms of a different coupling mechanism. A satisfactory explanation for our anomaly is to assume that electromagnetic emissions, including the 216 kHz frequency, were generated during the pre-seismic phase in the epicentral area (Biagi P.F., 1999; Molchanov et al., 1995) and superimposed with the MCO radio signal in the area of the receiver. Thus, the MCO radio signal intensity could increase.

The following recently published results appear to enhance the proposed genesis of the recorded radio anomaly (Potirakis et al., 2015): approximately 5–6 days before the Crete earthquake, the Vamos station (located in Chania prefecture) recorded a MHz EM anomaly. The analysis of this specific MHz EM time-series, which used both the method of critical fluctuations (MCF) (Contoyiannis and Diakonos, 2000, 2002) and the natural-time method (Varotsos et al., 2011), reveals "critical features" that imply that the possibly related underlying geophysical process is at a critical state. To strengthen this hypothesis, the seismicity of the area around the earthquake epicentre was also analysed. If the recorded EM signal is related to the preparation process of the Crete earthquake, it should present similar critical features with the recorded seismic activity prior to the main shock as different observable manifestations of the same complex system at critical state. Indeed, using the natural-time analysis, it was found that the foreshock activity also presents a critical characteristic, which confirms the hypothesis of the possible relation of the recorded MHz EM anomaly with the subsequent Crete earthquake.

It is noted that the pre-seismic MHz EM emission is considered to originate when a part of the Earth's crust fractured, which is characterized by high heterogeneity surrounding the family of large high-strength entities along the main fault of the system (Contoyiannis et al., 2005; Potirakis et al., 2013; Eftaxias and Potirakis, 2013 and references therein; Contoyiannis et al., 2015).

The traceability of EM potential precursors is considered problematic because they should normally be absorbed by the Earth's crust (Eftaxias and Potirakis, 2013 and references therein). Importantly, for an earthquake of approximately magnitude 6, the corresponding fracture process extends to a radius of approximately 120 km in terms of criticality. In addition, the MCF method reveals the critical window, during which any two active parts of the system are highly correlated at arbitrary long distances, whereas the fracture is non-directional (symmetry-breaking) (Contoyiannis et al., 2005). The aforementioned facts justify the observation of a fracture-induced EM anomaly, which is associated with an earthquake near the coastline, as occurred in the case under study. The fracture process during this stage of earthquake preparation is extended to the surface of the near land. Thus, the traceability of the associated EM emissions is not problematic.

The silence of the recorded MHz and radio anomalies prior to the earthquake occurrence is also justified in the framework of the aforementioned approach. The non-critical window appears in the MHz EM time-series after the appearance of the critical window. This phenomenon indicates that (i) a short-range correlation between the cracking events has emerged; (ii) the fracture process transitions from the phase of non-directional, almost symmetrical cracking distribution to a directional localized cracking zone, which is restricted along the main fault (symmetry breaking). The integration of symmetry breaking implies that the rupture process is obstructed along the backbone of strong asperities that sustain the fault surfaces. The "siege" of asperities has already begun. The traceability of the EM potential precursors beyond this point is considered problematic because they should normally be absorbed by the Earth's crust, except in the case of an earthquake that: (i) occurs in land, (ii) is strong, i.e., with magnitude of 6 or larger, and (iii) is shallow. In the present case, the focal depth is 40 km. In summary, the association of the observed anomaly with the stage of fracture of a heterogeneous region that surrounds the main fault appears justified, whereas its association with the focal area is problematic.

Finally, a recent paper (Vallianatos et al., 2014) describes in details the complexity of seismicity for the earthquake under consideration. Using non-extensive statistics, the magnitude distribution of the 2013 seismicity in the South West part of the Hellenic Arc was analysed for a time period before the main event. The analysis of the frequency magnitude (energy) distribution indicates an increase in degree of out-of-equilibrium state 2 days before the earthquake occurred. Moreover, the natural-time analysis shows that foreshock seismicity approached the critical stage, several days before the main event occurred. The LF radio anomalies are presented in this study for the first time for an event whose seismic complexity has been described. These results support the idea that there is a preparatory phase of an earthquake, which can affect various parameters.

6. Conclusions

Before the occurrence of the $M_w = 6.5$ Crete earthquake, an anomalous variation appeared in the intensity of an LF (216 kHz) radio signal sampled by a receiver located near the epicentre. After excluding faulty running of the transmitter and receiver, adverse meteorological conditions and abnormal geomagnetic activity, using a statistical analysis, we have demonstrated that the earthquake and radio anomaly are unlikely to be two unrelated events. Thus, the radio anomaly in this study helps increasing the number of successes in the field of the seismic precursors. The anomaly appeared 7 days before the earthquake, which is in the range of reported precursor times in the literature relative to radio anomalies. These anomalies are in the class of the so-called short-time precursors. The anomaly appears as an increase in radio signal intensity, which is difficult to justify with disturbances in the ionosphere-lower atmosphere during the preparatory phase of an earthquake; in fact, such disturbances would decrease the radio signal intensity. A satisfactory explanation is the electromagnetic emissions, which include the MCO (216 kHz) frequency, that are generated during the pre-seismic phase in the epicentral area. This possibility appears to be confirmed by recently published results on anomalous MHZ electromagnetic signals in the northwestern region of Crete in the same period.

Acknowledgements

The authors would like to acknowledge the two anonymous referees for useful comments and suggestions that have improved the overall quality of the present manuscript.

References

Alperovitch, L., 1997. Perturbation of atmospheric conductivity as a cause of the seismo-ionospheric interaction. Ann. Geophys. 15 (Suppl. 1). Abstract - XXII EGS Gen. Assembly, Vienna, Austria, April 1997.

Biagi, P.F., 1999. Seismic effects on LF radiowaves. In: Hayakawa, M. (Ed.), Atmospheric and Ionospheric Electromagnetic Phenomena Associated with Earthquakes. TERRAPUB, Tokyo, pp. 535–542.

Biagi, P.F., Piccolo, R., Ermini, A., Martellucci, S., Bellecci, C., Hayakawa, M., Capozzi, V., Kingsley, S.P., 2001a. Possible earthquake precursors revealed by LF radio signals. Nat. Hazards Earth Syst. Sci. 1 (1–2).

Biagi, P.F., Piccolo, R., Ermini, A., Martellucci, S., Bellecci, C., Hayakawa, M., Kingsley, S.P., 2001b. Disturbances in LF radio-signals as seismic precursors.

Please cite this article in press as: Maggipinto, T., et al., The LF radio anomaly observed before the $M_w = 6.5$ earthquake in Crete on October 12, 2013, Physics and Chemistry of the Earth (2015), http://dx.doi.org/10.1016/j.pce.2015.10.010

Ann. Geofis. 44, 5/6.
Biagi, P.F., Hayakawa, M., 2002. Possible premonitory behaviour of LF radiowaves on the occasion of the Slovenia earthquakes (M= 5.2-6.0-5.1) occurred on March-May 1998. In: Hayakawa, M., Molchanov, O. (Eds.), Seismo Electromagnetics: Lithosphere-atmosphere-ionosphere Coupling. TERRAPUB, Tokyo, pp. 249–253.
Biagi, P.F., Castellana, L., Maggipinto, T., Piccolo, R., Minafra, A., Ermini, A., Martellucci, S., Bellecci, C., Perna, G., Capozzi, V., Molchanov, O.A., Hayakawa, M., 2005. A possible preseismic anomaly in the ground wave of a radio broadcasting (216 kHz) during July-August 1998 (Italy). Nat. Hazards Earth Syst. Sci. 5, 727–732.
Biagi, P.F., Castellana, L., Maggipinto, T., Piccolo, R., Minafra, A., Ermini, A., Martellucci, S., Bellecci, C., Perna, G., Capozzi, V., Molchanov, O.A., Hayakawa, M., 2006. LF radio anomalies revealed in Italy by the Wavelet analysis: Possibile preseismic effects during 1997–1998. Phys. Chem. Earth 31, 403–408.
Biagi, P.F., Castellana, L., Maggipinto, T., Loiacono, D., Augelli, V., Schiavulli, L., Ermini, A., Capozzi, V., Solovieva, M.S., Rozhnoi, A.A., Molchanov, O.A., Hayakawa, M., 2008. Disturbances in a VLF radio signal prior the M=4.7 offshore Anzio (central Italy) earthquake on August 22, 2005. Nat. Hazards Earth Syst. Sci. 8, 1041–1048.
Contoyiannis, Y.F., Diakonos, F.K., 2000. Criticality and intermittency in the order parameter space. Phys. Lett. A 268 (4–6), 286–292.
Contoyiannis, Y.F., Diakonos, F.K., Malakis, A., 2002. Intermittent dynamics of critical fluctuations. Phys. Rev. Lett. 89 (035701).
Contoyiannis, Y.F., Kapiris, P.G., Eftaxias, K.A., 2005. Monitoring of a preseismic phase from its electromagnetic precursors. Phys. Rev. E 71 (066123).
Contoyiannis, Y.F., Potirakis, S.M., Eftaxias, K., Contoyianni, L., 2015. Tricritical crossover in earthquake preparation by analyzing preseismic electromagnetic emissions. J. Geodyn. me 84, 40–54.
Daubechies, I., 1992. .: Ten Lectures on Wavelets, CBMS – NSF Regional Conferences Series in Applied Mathematics. SIAM, Philadelphia PA, p. 61.
Eftaxias, K., Potirakis, S.M., 2013. Current challenges for pre-earthquake electromagnetic emissions: shedding light from micro-scale plastic flow, granular packings, phase transitions and self-affinity notion of fracture process. Nonlinear Process. Geophys. 20 (issue 5), 771–792.
Hayakawa, M., Sato, H., 1994. Ionospheric perturbations associated with earthquakes, as detected by subionospheric VLF propagation. In: Hayakawa, M., Fujinawa, Y. (Eds.), Electromagnetic Phenomena Related to Earthquake Prediction. TERRAPUB, Tokyo, pp. 391–397.
Hayakawa, M., Molchanov, O.A., Ondoh, T., Kawai, E., 1996. The precursory signature effect of the Kobe earthquake on subionospheric VLF signals. J. Commun. Res. Laboratory 43, 169–180.
Hayakawa, M., Ohta, K., Maekawa, S., Yamauchi, T., Ida, Y., Gotoh, T., Yonaiguchi, N., Sasaki, H., Nakamura, T., 2006. Electromagnetic precursors to the 2004 Mid Niigata Prefecture earthquake. Phys. Chem. Earth 31, 356–364.
Hayakawa, M., Kasahara, Y., Nakamura, T., Muto, F., Horie, T., Maekawa, S., Hobara, Y., Rozhnoi, A.A., Solovieva, M., Molchanov, O.A., 2010. A statistical study on the correlation between lower ionospheric perturbations as seen by subionospheric VLF/LF propagation and earthquakes. J. Geophys. Res. 115, A09305. http://dx.doi.org/10.1029/2009JA015143.
Molchanov, O.A., Hayakawa, M., Rafalsky, V.A., 1995. Penetration characteristics of electromagnetic emissions from an underground seismic source into the atmosphere, ionosphere, and magnetosphere. J. Geophys. Res. 100 (Issue A2), 1691–1712.
Molchanov, O.A., Hayakawa, M., 1998. Subionospheric VLF signal perturbations possibly related to earthquakes. J. Geophys. Res. 103, 17489–17504.
Molchanov, O.A., Rozhnoi, A., Solovieva, M., Akentieva, O., Berthelier, J.J., Parrot, M., Lefeuvre, F., Biagi, P.F., Castellana, L., Hayakawa, M., 2006. Global diagnostic of the ionospheric perturbations related to the seismic activity using the VLF radio-signals collected on the Demeter satellite. Nat. Hazards Earth Syst. Sci. 6, 745–753.
Morgounov, V.A., Ondoh, T., Nagai, S., 1994. Anomalous variation of VLF signals associated with strong earthquakes (M≥7.0). In: Hayakawa, M., Fujinawa, Y. (Eds.), Electromagnetic Phenomena Related to Earthquake Prediction. TERRAPUB, Tokyo, pp. 409–428.
Papazachos, B.C., Delibasis, N.D., 1969. Tectonic stress field and seismic faulting in the area of Greece. Tectonophysics 7, 231–255.
Papazachos, B.C., Comninakis, P.E., 1970. Geophysical features of the Greek Island Arc and Eastern Mediterranean Ridge. In: Com. Rend. des Seances de la Conf. Reunie a Madrid, vol. 16, pp. 74–75.
Papazachos, B.C., Comninakis, P.E., 1971. Geophysical and tectonic features of the Aegean arc. J. Geophys. Res. 76, 8517–8533.
Papazachos, B.C., Papazachou, C., 2003. The Earthquakes of Greece. Ziti Publications, Thessaloniki, p. 317.
Papazachos, B.C., Karakostas, B.G., Papazachos, C.B., Scordilis, E.M., 2000. The geometry of the Benioff zone and lithospheric kinematics in the Hellenic Arc. Tectonophysics 319, 275–300.
Pirazzoli, P.A., Thomeret, J., Thomeret, Y., Laborel, J., Montagionni, L., 1982. Crustal block movements from Holocene shorelines: Crete and Antikythira (Greece). Tectonophysics 68, 27–43.
Potirakis, S.M., Contoyiannis, Y., Eftaxias, K., Koulouras, G., Nomicos, C., 2015. Recent field observations indicating an Earth system in critical condition before the occurrence of a significant earthquake. IEEE Geoscience Remote Sens. Lett. 12 (issue 3), 631–635. http://dx.doi.org/10.1109/LGRS.2014.2354374.
Potirakis, S.M., Karadimitrakis, A., Eftaxias, K., 2013. Natural time analysis of critical phenomena: the case of pre-fracture electromagnetic emissions. Chaos 23 (023117).
Pulinets, S.A., Hegai, V.V., Boyarchuk, K.A., Alekseev, V.A., 1998. The new conception of earthquake prediction. Ann. Geophys 16 (Suppl. 1). Abstract - XXIII EGS General Assembly, Nice, France, April 1998.
Rozhnoi, A., Solovieva, M.S., Molchanov, O.A., Hayakawa, M., 2004. Middle latitude LF (40 kHz) phase variations associated with earthquakes for quiet and disturbed geomagnetic conditions. Phys. Chem. Earth 29, 589–598.
Rozhnoi, A.A., Solovieva, M.S., Molchanov, O.A., Hayakawa, M., Maekawa, S., Biagi, P.F., 2005. Anomalies of LF signal during seismic activity in November–December 2004. Nat. Hazards Earth Syst. Sci. 5, 657–660.
Rozhnoi, A.A., Solovieva, M.S., Molchanov, O.A., Chebrov, V., Voropaev, V., Hayakawa, M., Maekawa, S., Biagi, P.F., 2006. Preseismic anomaly of LF signal on the wave path Japan-Kamchatka during November 2004. Phys. Chem. Earth 31, 422–427.
Rozhnoi, A., Molchanov, O., Solovieva, M., Gladyshev, V., Akentieva, O., Berthelier, J.J., Parrot, M., Lefeuvre, F., Hayakawa, M., Castellana, L., Biagi, P.F., 2007. Possible seismo-ionosphere perturbations revealed by VLF signals collected on ground and on a satellite. Nat. Hazards Earth Syst. Sci. 7, 617–624.
Strang, G., Nguye, T., 1996. Wavelets and Filter Banks. Wellesley Cambridge Press, p. 490.
Torrence, C., Compo, G.P., 1998. A practical guide to wavelet analysis. Bull. Am. Meteorological Soc. 79 (1), 61–78.
Thommeret, Y., Laborel, J., Montaggioni, L., Pirazzoli, P., 1981. Late Holocene shoreline changes and seismotectonic displacements in western Greece (Greece). Z. Geomorphol. 127–149. Supplement Issues, 40.
Vallianatos, F., Michas, G., Papadakis, G., 2014. Non-extensive and natural time analysis of seismicity before the Mw6.4, October 12, 2013 earthquake in the South West segment of the Hellenic Arc. Phys. A Stat. Mech. Appl. 414, 163–173.
Varotsos, P., Sarlis, N.P., Skordas, E.S., Uyeda, S., Kamogawa, M., 2011. Natural time analysis of critical phenomena. PNAS 108 (28), 11361–11364.

Please cite this article in press as: Maggipinto, T., et al., The LF radio anomaly observed before the $M_w = 6.5$ earthquake in Crete on October 12, 2013, Physics and Chemistry of the Earth (2015), http://dx.doi.org/10.1016/j.pce.2015.10.010